DOI 10.1002/pmic.201500515 *Proteomics* 2016, *16*, 1660–1669

RESEARCH ARTICLE

Protein biomarkers on tissue as imaged via MALDI mass spectrometry: A systematic approach to study the limits of detection

Stephanie M. W. Y. van de Ven[1,2], Kyle D. Bemis[3], Kenneth Lau[1], Ravali Adusumilli[1,2], Uma Kota[1,4], Mark Stolowitz[1,2], Olga Vitek[5], Parag Mallick[1,2] and Sanjiv S. Gambhir[1,2,6,7]

[1] Canary Center at Stanford, Department of Radiology, Stanford University School of Medicine, Stanford, CA, USA
[2] Molecular Imaging Program at Stanford, Stanford University School of Medicine, Stanford, CA, USA
[3] Department of Statistics, Purdue University, West Lafayette, IN, USA
[4] Thermo Fisher Scientific, San Jose, CA, USA
[5] College of Science, College of Computer and Information Science, Northeastern University, Boston, MA, USA
[6] Department of Bioengineering, Stanford University School of Medicine, Stanford, CA, USA
[7] Department of Materials Science & Engineering, Stanford, CA, USA

MALDI mass spectrometry imaging (MSI) is emerging as a tool for protein and peptide imaging across tissue sections. Despite extensive study, there does not yet exist a baseline study evaluating the potential capabilities for this technique to detect diverse proteins in tissue sections. In this study, we developed a systematic approach for characterizing MALDI-MSI workflows in terms of limits of detection, coefficients of variation, spatial resolution, and the identification of endogenous tissue proteins. Our goal was to quantify these figures of merit for a number of different proteins and peptides, in order to gain more insight in the feasibility of protein biomarker discovery efforts using this technique. Control proteins and peptides were deposited in serial dilutions on thinly sectioned mouse xenograft tissue. Using our experimental setup, coefficients of variation were <30% on tissue sections and spatial resolution was 200 μm (or greater). Limits of detection for proteins and peptides on tissue were in the micromolar to millimolar range. Protein identification was only possible for proteins present in high abundance in the tissue. These results provide a baseline for the application of MALDI-MSI towards the discovery of new candidate biomarkers and a new benchmarking strategy that can be used for comparing diverse MALDI-MSI workflows.

Received: December 10, 2015
Revised: February 23, 2016
Accepted: March 5, 2016

Keywords:
Limit of detection / MALDI Imaging / Mass spectrometry / Protein biomarkers / Sensitivity / Technology

Additional supporting information may be found in the online version of this article at the publisher's web-site

1 Introduction

MALDI mass spectrometry imaging (MSI) is an emerging technique for the analysis of proteins and peptides as well as other analytes, such as lipids and drugs, across tissue sections. It is a label-free method that may ultimately provide powerful information on the spatial distribution of multiple compounds simultaneously [1–3], and it complements other MSI workflows including desorption electrospray ionization

Correspondence: Dr. Sanjiv S. Gambhir, MD, PhD, Chair, Department of Radiology, Director, Molecular Imaging Program at Stanford (MIPS), Director, Canary Center at Stanford, Professor, Department of Radiology, Department of Bioengineering, and Department of Materials Science & Engineering, The James H Clark Center, 318 Campus Drive, East Wing, 1st Floor, Stanford, CA 94305–5427, USA
E-mail: sgambhir@stanford.edu
Fax: +1-650-724-4948

Abbreviations: EGFR, epidermal growth factor receptor; **MALDI-MSI**, matrix assisted laser desorption ionization mass spectrometry imaging; **ROI**, region of interests

Colour Online: See the article online to view Figs. 2–5 in colour.

Significance of the study

We developed a novel systematic approach to characterize MALDI-MSI workflows in terms of limits of detection, coefficients of variation, spatial resolution, and the identification of endogenous tissue proteins. These results provide a baseline for the application of MALDI-MSI towards the discovery of new candidate biomarkers. Moreover, our systematic approach affords a new benchmarking strategy that can be used for comparing diverse MALDI-MSI workflows. This new approach may improve current workflows and aid in achieving the improvements in protein detection required for clinical biomarker discovery.

mass spectrometry imaging and secondary ion mass spectrometry imaging [4, 5]. MALDI-MSI has been used for classification of different tissue regions, such as cancer versus non-cancer, by comparing endogenous protein/peptide MS profiles of these tissue types [6,7]. One of the goals of MALDI-MSI approaches is to use the information in these spatially resolved profiles for discovery of new protein biomarkers that could advance the detection and treatment of difficult-to-treat diseases in the future.

In the typical MALDI-MSI workflow, flash frozen tissue is sectioned into thin slices and thaw-mounted onto conductive slides. After washing of the tissue sections, a MALDI matrix is applied to assist in desorption and ionization of the molecules. A two-dimensional array of MALDI mass spectra is then acquired, with each spectrum representing a spatial location on the sample. Specialized software is used to process and visualize the signals in the data. A common next step is the identification of protein identities from the spectra. This is an important and non-trivial process, requiring several additional experimental steps including tryptic digestion, MS/MS, and correction of mass shifts using internal calibrants [8, 9].

In order to characterize differences between tissue types, several MALDI-MSI studies have focused on classifying unknown peaks [7, 10–16], yet this is fundamentally different from identifying or discovering specific analytes, which requires more complex processes that can limit sensitivity. In principle, the quantitative information derived from mass spectra can characterize underlying differences in spatial and biochemical composition of tissues more fully, but thus far the quantitative capabilities of MALDI-MSI are insufficiently characterized in terms of LOD, LOQ, limits of identification and spatial resolution. In addition, the relationship between these capabilities and the attributes of tissue sections (e.g. typical protein concentrations and feature spacing) has not been clearly established. A few groups have used MALDI-MSI to quantify small molecules in tissue [17–20]. Of these groups, Groseclose et al. reported an LOD for Lapatinib of 616 ng/g of tissue [17], and Koeniger and colleagues found an LOD of 2.4 nM for Olanzapine [19]. For proteins, however, this has not been addressed thus far. Determining these figures of merit for proteins in tissue is essential in choosing relevant applications for this technique, and in determining if protein biomarker discovery efforts using MALDI-MSI are worthwhile. Protein quantification in tissue sections was shown by Clemis et al. using a different imaging strategy, MALDI multiple reaction monitoring (MRM) MS [21]. They demonstrated detection of myelin basic protein in rat brains at concentrations of 0.001–0.071 amol/μm^3 (1–70 μM). Their method involved in situ tryptic digestion followed by deposition of an isotopically labeled standard peptide from the target protein onto the tissue. The ratio of MRM transitions for the endogenous unlabeled proteolytic peptide to the deposited isotopically labeled standard peptide was used for peptide quantitation. Clemis and colleagues used a *targeted* imaging approach, not a typical MALDI-MSI method, and their strategy has limitations with regards to quantification of more than one protein per tissue section.

In this study we developed a systematic approach for evaluating the LOD, LOQ, limits of identification and spatial resolution of a set of proteins on both simple and complex matrices using a typical MALDI-MSI workflow. Our goal was to quantify these figures of merit of MALDI-MSI for a number of different proteins and peptides. As far as we know, this is the first study that provides a systematic approach to study the sensitivity of MALDI-MSI for protein detection on tissue.

2 Materials and methods

All animal procedures were conducted per protocol 21637, approved by the Stanford University Administrative Panels on Laboratory Animal Care.

2.1 Reagents

Peptide and protein standards, proteomics grade trypsin, and MALDI matrices were obtained from Sigma-Aldrich (St. Louis, MO). α-cyano-4-hydroxycinnamic acid (CHCA) was used for (tryptic) peptide analyses (10 mg/mL in 50% acetonitrile and 0.1% trifluoroacetic acid (TFA)), and sinapinic acid (SA) was used for intact protein analyses (20 mg/mL in 50% acetonitrile and 0.1% TFA). The following protein and peptide standards were used: Angiotensin II (human), Cytochrome c (equine), Apomyoglobin (equine). These standards were selected because they are well characterized and known to ionize well. Moreover, because these proteins and

peptides were not present in the xenograft tissues, potential interference of endogenous levels of these proteins was not a concern for our LOD evaluations. Standards were used in concentration ranges of 0.084 to 420 pm/μL to determine LOD.

2.2 Tissue and slide preparation

A431 xenograft tissues established in nude mice were used for the dilution series of proteins and peptides. The generation of these xenografts has previously been described [22]. Tissues were flash frozen in liquid nitrogen immediately after excision and stored at −80°C. For MALDI imaging, 10 μm sections were cut by Cryomicrotome (Leica CM1850, Wetzlar, Germany) using minimal optimum cutting temperature (OCT) embedding and thaw-mounted directly onto indium-tin-oxide coated slides (SPI Supplies, West Chester, PA). The slides with tissue sections were then washed and fixed in graded isopropanol and water to remove the OCT (70 and 95% isopropanol for 30 s each, followed by ten dips in ultrapure water, and then repeated isopropanol washing) [23].

2.3 Deposition of reagents

Two systems were tested for the deposition of reagents, an acoustic robotic spotter (Portrait 630, LabCyte Inc., Sunnyvale, CA, USA) and a sprayer (SunCollect, SunChrom, Friedrichsdorf, Germany). The acoustic robotic spotter uses a focused acoustic ejector to produce droplets of 170 pL. A detailed report of the operational characteristics has been presented elsewhere [24]. The sprayer uses pneumatic atomization to spray homogenous layers of reagent onto a predefined area. First, we assessed the variation in reagent deposition using the Portrait spotter and the Sunchrom sprayer under various conditions, performing each experiment at least three times. We mixed a protein (Cytochrome c) and a fluorophore (Alexa Fluor 680, Life Technologies) at 84 pm/μL in 50% acetonitrile and 0.1% TFA to measure the variance in fluorescent signal after deposition on a slide and on a tissue section using a fluorescent microscope (Olympus IX81). After determining the variation in deposition for both systems, we then continued to use the acoustic robotic spotter for the rest of our experiments. Reagent deposition parameters are described in Table 1.

Proteins and peptides were diluted in the desired concentration ranges in 50% acetonitrile and 0.1% TFA to a total volume of 500 μL to fill the reservoir of the robotic spotter. The serial dilutions were then deposited on the slide and on the tissue in six (Angiotensin II) or seven (Cytochrome c and Apomyoglobin) cycles of one 170 pL droplet per cycle. Spacing between individual spots was 280 μm or more and proteins and peptides were deposited in blocks of 6×6 or 8×8 spots. After deposition, the spots were allowed to dry before any matrix or trypsin was spotted on top of them, mimicking

Table 1. Methods overview

Experiment	LOD peptide	LOD intact protein	LOD in situ tryptic digest	Deposition spotter	Deposition sprayer	Spatial resolution intact protein	Spatial resolution in situ tryptic digest	Endogenous proteins
Protein/peptide deposition	Angiotensin II	Apomyoglobin, Cytochrome c	Apomyoglobin, Cytochrome c	Cytochrome c	Cytochrome c	Cytochrome c	Cytochrome c	–
Cycles protein/peptide solution	6	7	7	7	7 (7.5 μL/min)	7	7	–
Cycles trypsin solution	–	–	30 (over 2 hours)	–	–	–	30 (over 2 hours)	30 (over 2 h)
Matrix	CHCA (10 mg/mL)	SA (20 mg/mL)	CHCA (10 mg/mL)	–	–	SA (20 mg/mL)	CHCA (10 mg/mL)	CHCA (10 mg/mL)
Cycles matrix	10	10	30	–	–	10	30	30
Number of spots (x * y)	6–8 * 6–8	6-8 * 6–8	6-8 * 6–8	6 * 6	–	1, 2, and 3 * 4 spot features	1, 2, and 3 * 4 spot features	~40 * 40 (entire tissue)
m/z range	900–4000	5000—25 000	900–4000	–	–	5000–25 000	900–4,000	900 - 4,000
Spots spacing (μm)	280	280	280	280	–	120–320	200–400	280

a scenario in which a tissue section of interest would contain a certain amount of protein or peptide on its surface.

In situ trypsin digestion was performed following the protocol by Casadonte and Caprioli [25], and further optimized in our laboratory setting. Trypsin solution (0.08 μg/μL in 100 mM ammoniumbicarbonate and 10% acetonitrile) was deposited in 30 cycles (5 nL total volume) with a repeat time between cycles of 180 s to allow for sufficient incubation of the trypsin solution on the tissue/slide. CHCA matrix (10 mg/mL) was deposited in 30 cycles also. Instrument calibration was performed every 60 min and when necessary.

2.4 Patterns for spatial resolution

To determine the spatial resolution of our instrumental setup, we developed patterns (line, rectangle, square) for the acoustic robotic spotter. We tested these patterns by depositing intact protein at a fixed concentration (Cytochrome c at 420 pm/μL) on the slides and tissue surfaces while varying the distance from pattern to pattern. We acquired the MALDI imaging signals from the intact proteins and the peptides resulting from in situ trypsin digestion. We measured the smallest distance at which two patterns could be discriminated as separate to determine the spatial resolution of this technique.

2.5 Fluorescent microscopy imaging

Fluorescent images were acquired using Metamorph software (Version 7.8.4.0, Universal Imaging Corp., West Chester, PA) and an Olympus IX81 microscope (Olympus, PA, USA) attached to an Orca-R2 digital camera (Hamamatsu Photonics, Hamamatsu, Japan). The Cy5 filter set and the 4x objective were used; exposure times were 0.3 s on the tissue and 1 s on the slide. ImageJ 1.46r (National Institutes of Health, USA) was used for analysis of the fluorescent microscopy images. After color threshold adjustment, region of interests (ROIs) outlining the fluorescent spots (deposited by the acoustic robotic spotter) were created using the function 'analyze particles'. These ROIs were then saved and used to measure the integrated density values on the original microscopy images. The fluorescent images acquired after protein deposition with the sprayer were also analyzed using the same ROIs.

2.6 MALDI mass spectrometry imaging

After deposition of reagents, the slides on the MALDI target plate were imaged on a digital flatbed scanner first (HP Scanjet 5590), and this image was then imported in the AB SCIEX TOF/TOF Imaging Software package to guide MS image acquisition on the AB SCIEX TOF/TOF 5800 System (AB SCIEX, Framingham, MA). Intact protein data was acquired in linear positive mode with a mass range of 5000–25 000 m/z; (tryptic) peptide data was acquired in reflectron positive mode with a mass range of 900–4000 m/z; 600 laser shots were taken per pixel at a spatial resolution of 100 μm.

2.7 MALDI-MSI data analysis

CARDINAL MS image analysis software (http://www.cardinalmsi.org/) was used to view and analyze the MALDI-MSI data [26]. For the dilution experiments, an ROI was drawn around each block (of six to eight by six to eight spots) and the mean signal intensity and standard error was calculated for the peaks of interest after normalizing the spectra to total ion current. GraphPad Prism 6 (Version 6.0d, GraphPad Software Inc., CA, USA) was used to calculate linear regression curves based on the mean intensities of the serial dilutions in three repeated measurements. The LOD was defined as the smallest amount of protein/peptide per spot with a significantly higher signal (at a 95% confidence level) than the control spots (only matrix with no protein/peptide deposited).

The coefficient of variation was defined as the standard error compared to the mean signal intensity of the ROI. Each experiment was repeated at least twice.

2.8 Protein identification

Tissue sections adjacent to the ones used for MALDI-MSI were processed to identify proteins by in solution tryptic digestion, followed by LC-MALDI using the Tempo™ LC MALDI Spotting System and the TOF/TOF 5800 System (AB SCIEX, Framingham, MA). The Mascot search engine (Matrix Science, USA) was used to search the data files in the UniProtKB/Swiss-Prot database. Peaks found by LC-MALDI were compared to peaks found by MALDI-MSI, using an internal calibrant to increase confidence in peptide matching between the two methods [8]. MS/MS was also performed directly on the tissue sections after in situ tryptic digestion to accurately identify endogenous proteins. We used inclusion lists to increase our potential to identify specific proteins: proteins of high and medium abundance (based on spectral count data) were compared.

A schematic overview of our study's workflow is shown in Fig. 1.

3 Results

We developed a systematic approach for characterizing MALDI-MSI workflows in terms of LOD, LOQ, limits of identification and spatial resolution (Fig. 1). We quantified the various attributes of a MALDI-MSI workflow performed in our lab for a set of proteins on both simple (conductive slides) and complex (tissue sections) matrices, in order to gain more insight in the feasibility of protein biomarker discovery using this technique.

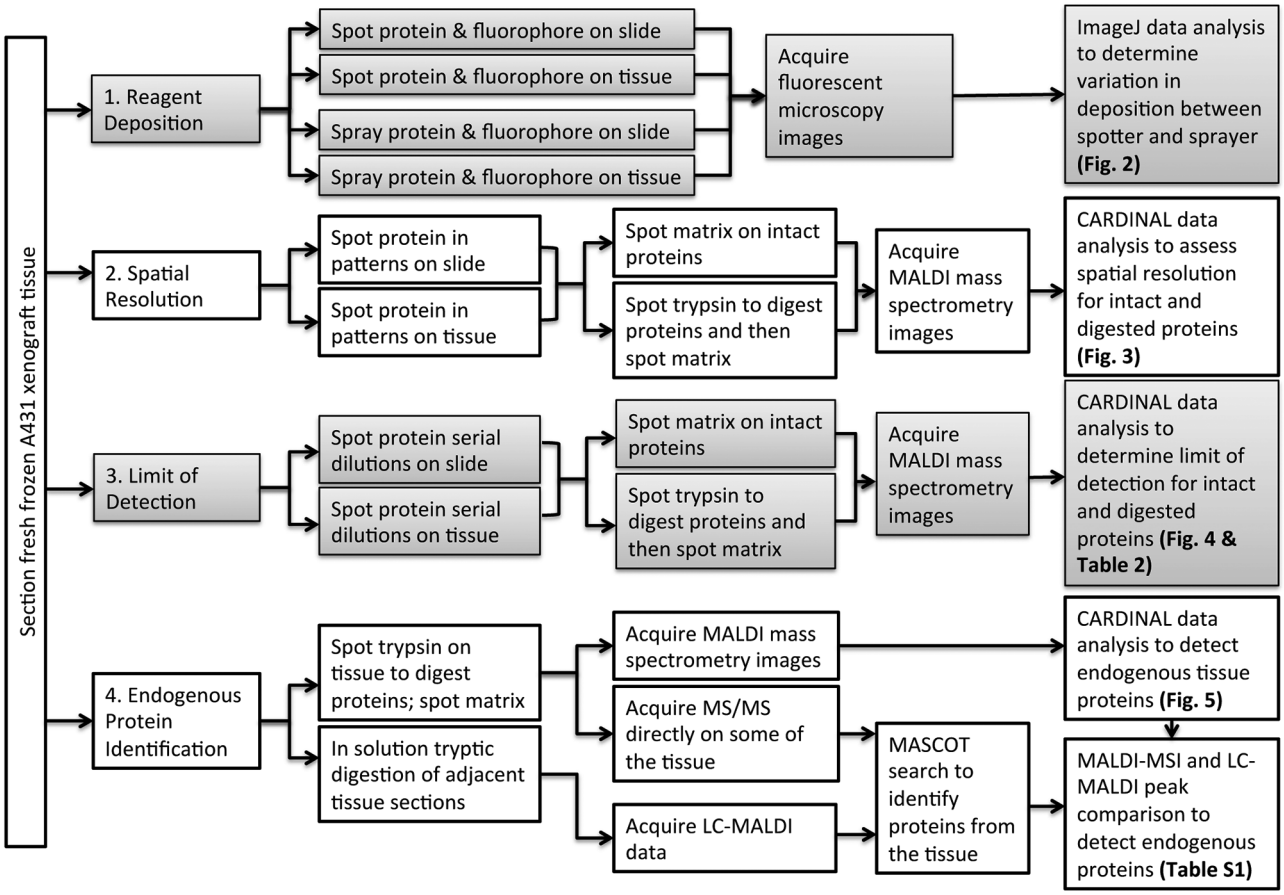

Figure 1. Workflow used in this study for the assessment of reagent deposition, spatial resolution, limit of detection, and endogenous protein detection.

3.1 Variation in reagent deposition is smallest using robotic spotter

We compared a robotic spotter and a sprayer to determine the uniformity of reagent deposition for each instrument. Coefficient of variation (CV) using the robotic spotter was 22% on tissue and 58% on slide; using the sprayer the CV was 28% on tissue and 67% on slide (Fig. 2a–d). Since the robotic spotter showed slightly better results in terms of variation in deposition, and also gave us the ability to accurately deposit individual nano-droplets of protein solution onto a slide or tissue surface, we decided to use the robotic spotter for the remainder of the experiments described here.

3.2 Spatial resolution is highest for intact proteins

Intact protein (Cytochrome C at 420 pm/μL concentration) was deposited onto slides and onto tissue sections in three patterns (line, rectangle, square), while varying the spacing between the patterns. To determine the spatial resolution of our workflow, we measured the smallest distance at which two patterns could be discriminated. Since spatial resolution is instrument dependent, results reported here are specific to our instrumental setup. Figure 3 shows that in intact protein imaging discrimination of different features is possible when they are 200 μm apart (or more). Results for protein deposition directly on the slide and deposition on the tissue surface are the same. When in situ tryptic digestion of the proteins is performed, more spacing is needed between patterns in order to discriminate them (bottom half of Fig. 3). On a slide, two patterns can be discriminated at a distance of 360 μm. Because of the higher LOD due to the signal suppression we observed on tissue (also see Fig. 4), not all features spotted on the tissue surface were detectable in their entirety after in situ tryptic digestion. The distance needed to reliably discriminate patterns on the tissue surface is most probably similar to the distance needed on the slide (360 μm or more).

3.3 Limits of detection for proteins and peptides are in micromolar to millimolar range

We quantified the LOD of MALDI-MSI using serial dilutions of a number of different proteins and peptides on both simple and complex matrices using our MALDI-MSI workflow.

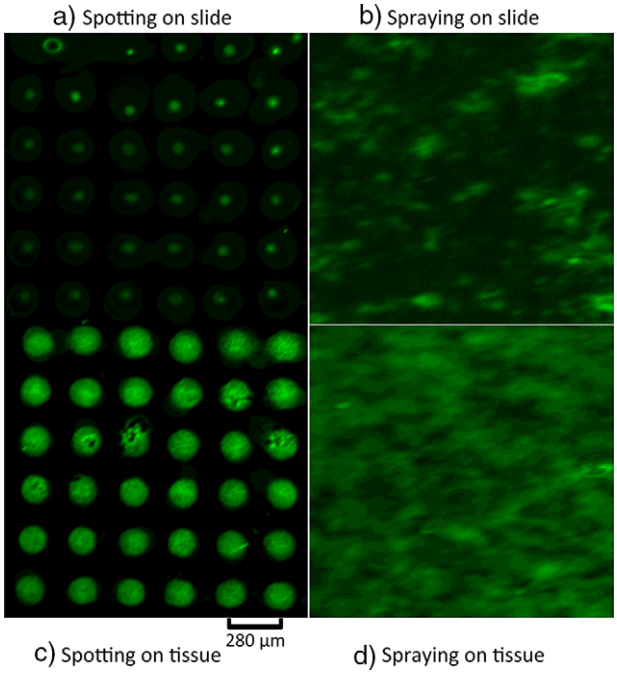

Figure 2. Measurements of variation in spotting versus spraying. A mixture of protein and fluorophore was deposited directly onto slides (a, b) and onto tissue sections (c, d). An acoustic robotic spotter (a, c) and a sprayer (b, d) were compared. Variation in fluorescent signal measurements was 58% (a), 67% (b), 22% (c), and 28% (d).

Figure 4 shows the MALDI-MS images of serial dilutions of apomyoglobin, imaged on a conductive slide and on a tissue section. The LOD in absolute amounts of apomyoglobin deposited was 2 fm when spotted directly onto a conductive slide, and 8 fm when spotted onto the tissue surface (mean signal intensity measured higher than background). Mean signal intensity was plotted against protein concentration (Fig. 4e). The signal suppression observed on tissue is illustrated in Fig. 4f, where the mass spectra of 16 fm apomyoglobin spots on the slide and the tissue surface are overlaid for comparison. Approximately, a ten-fold suppression in signal was observed across all spots on the tissue. For in situ tryptic digestion, more protein deposition was needed to detect the protein. On a slide, 5 fm of apomyoglobin was deposited per spot in order to detect the tryptic peptides by MALDI-MSI, whereas on a tissue surface, 500 fm of apomyoglobin was needed in order to be detectable (Table 2). LOD for the other proteins and peptides studied were comparable to these results (Table 2). CV ranged from 5 to 30% across the protein deposition experiments.

The above results are reported in absolute protein amounts (fm). To extrapolate these numbers to the detection of endogenous proteins from tissue sections by MALDI-MSI, we computed the lowest amount of protein per tissue volume needed for detection. Since each 150 μm diameter circular spot represents a tissue area, and since the tissue was sectioned at 10 μm thickness, this leads to a tissue volume per spot of $\sim 1.77 \times 10^{-7}$ mL. With an assumed tissue density of 1 g/mL, the molar LOD per tissue volume were computed. As seen from Table 2, the LOD are in the micromolar to millimolar range.

The amount of cells per spot varies with the composition of the tissue, but when assuming an average cell volume of $\sim 2200\ \mu m^3$ [27], approximately 80 cells would be present in the tissue volume under a 150 μm diameter spot. With an LOD of 8 fm/spot, this means that at least 0.1 fm of protein should be available per cell in order to be detectable, which corresponds to 60 million molecules per cell. As an example, the A431 cell line has a well-described overexpression of the epidermal growth factor receptor (EGFR), which was initially the reason we chose this model for evaluation of our MALDI-MSI strategy. The number of epidermal growth factor receptors per cell is approximately 2.8 million in this cell line [28], which is well below the LOD of this MALDI imaging strategy.

3.4 Endogenous protein identification in tissue is feasible for highly abundant proteins

We compared the list of precursors found after tryptic digestion and LC-MALDI of adjacent tissue sections with the list of peaks resulting from MALDI-MSI after *in situ* tryptic digestion. The detectable masses were limited to the top 5–10% of all proteins identified in the tissue (based on spectral count data), confirming our findings in the LOD experiments. When we used a mass tolerance of 0.1 Da for peptide matching and included peaks with signals above noise level (mean intensity ≥ 60), 192 peptide sequences of 89 proteins were detected (Supporting Information, S1 Table).

To demonstrate that in addition to matching precursor masses we can actually identify proteins directly from the mounted tissue, we performed MS/MS on tissue sections after *in situ* tryptic digestion. An example of this is shown in Fig. 5, where peptide VVSTHEQVLR from human Keratin, type I cytoskeletal 14 was identified by Mascot search after in situ MS/MS on tissue. This protein is highly abundant (top 1%) in human squamous cell carcinoma (A431 cells), allowing for detection by MALDI-MSI. As we expected from our LOD experiments however, medium abundance proteins such as EGFR (identified in the top 25% of proteins by LC-MALDI) were not detectable by MALDI-MSI.

Table 3 lists the main criteria we used to evaluate MALDI-MSI performance with regard to tissue imaging and summarizes our findings.

4 Discussion

We developed a systematic approach to study the sensitivity of MALDI-MSI for protein detection on tissue. Using this approach, we showed that the LOD for proteins on tissue using

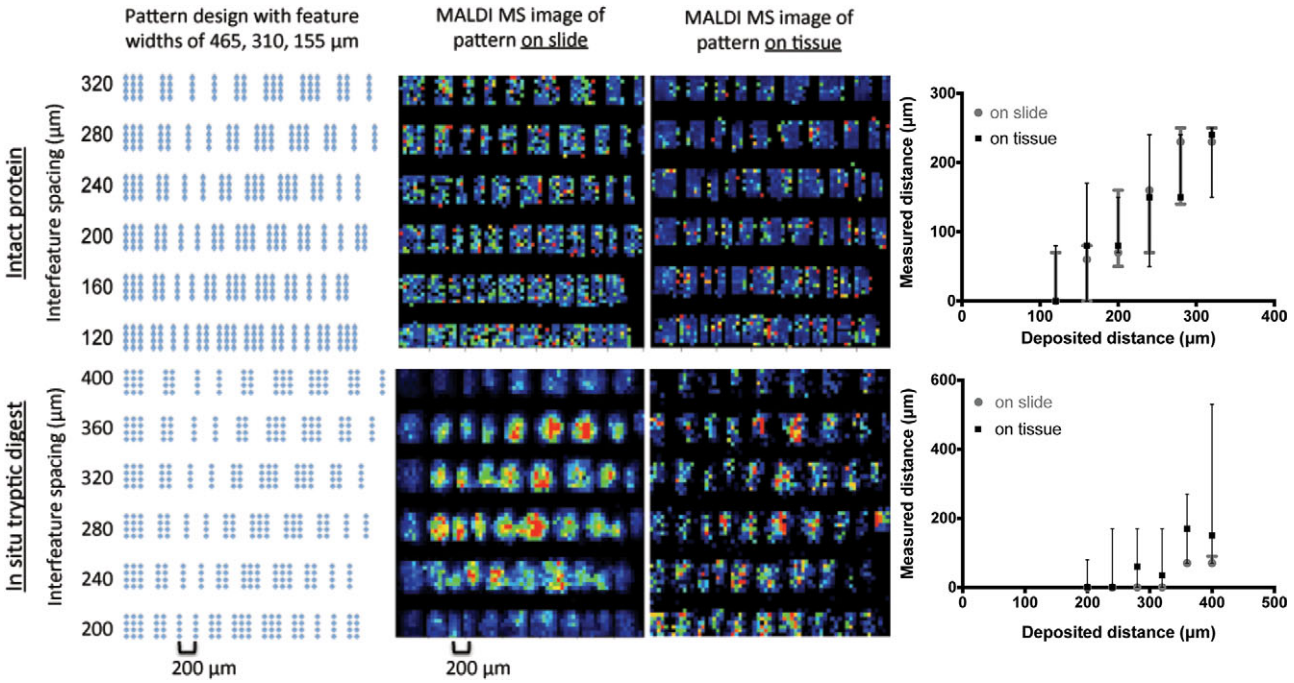

Figure 3. Spatial resolution measurements. Intact protein (Cytochrome C at 420 pm/µL concentration) was deposited onto slides and onto tissue sections in three patterns (line, rectangle, square), while varying the spacing between the patterns along the X axis. The intact protein was digested in situ using trypsin (bottom half of the Figure). MALDI imaging signals from intact proteins (top panels) and from in situ tryptic digests (bottom panels) were quantified; an *m/z* of 12359.7 was representative for the peak of intact Cytochrome C; an *m/z* of 1168.4 was representative for the Cytochrome C peptide TGPNLHGLFGR. The graphs on the right depict the medians and ranges of measured distances (µm) vs. deposited distances (µm) on slides and tissue sections. The smallest distance at which two features could reliably be discriminated was 200 µm for intact proteins and 360 µm for in situ tryptic digests.

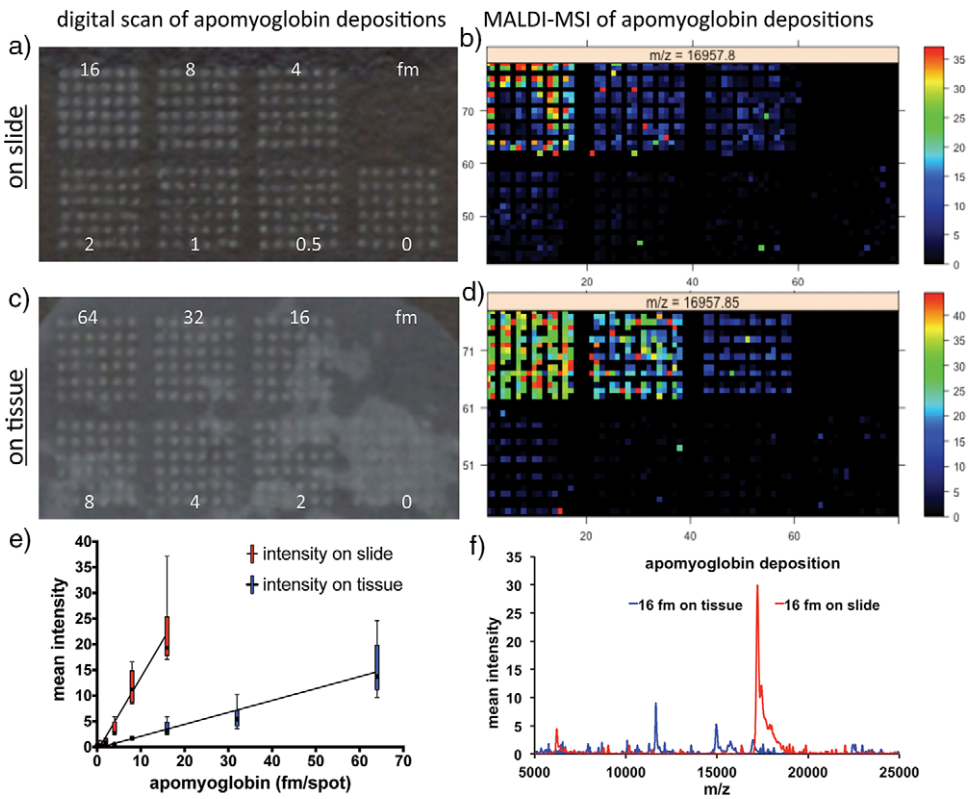

Figure 4. Limit of detection (LOD). Dilutions of apomyoglobin (between 0 and 64 fm/spot) were deposited onto slides (a, b) and onto tissue sections (c, d) in blocks of 6×6 spots. A digital scan (a, c) of the spots and their MALDI image (b, d) are shown. Mean signal intensity was plotted against protein concentration (e). Substantial (~10-fold) signal suppression was observed on tissue when comparing the same protein concentrations (f).

Table 2. Limit of detection (LOD) overview. Absolute amounts are given in femtomoles and amounts per tissue area in μM

Protein name (MW)	Condition	LOD on slide (fm)	LOD on tissue (fm)	LOD/tissue volume (μM)
Angiotensin II (1 kDa)	Intact	0.02	0.25	1.4
Apomyoglobin (17 kDa)	Intact	2	8	45
Cytochrome C (12 kDa)	Intact	5	25	141
Apomyoglobin (17 kDa)	Tryptic digest	5	500	2829
Cytochrome C (12 kDa)	Tryptic digest	2.5	100	566

MALDI-MSI with our methodology and instrumentation is in the micromolar to millimolar range.

These results emphasize the challenge of protein biomarker discovery with MALDI-MSI at its current stage of development for most applications. However, we believe that our results are in agreement with overall findings currently reported in literature. Comparisons across different platforms, sample preparation techniques, and tissue types are difficult, but proteins that have been identified thus far are predominantly highly abundant (top 5–10%). Examples of these confirmed proteins are hemoglobin subunits, actin, and histones. All of these were identified in this study, e.g. Histone H2A peptide (AGLQFPVGR, Table S1), which was also identified by Cole and colleagues [29]. Recently, Min and colleagues have identified ribosomal protein P2 in thyroid cancer tissue, which is also a highly abundant protein [30]. Maier et al. also reported that the protein biomarkers detected by MALDI-MSI are mainly abundant cellular proteins [9]. Although using a different, targeted imaging approach (MALDI-MRM), Clemis et al. detected the highly abundant myelin basic protein at micromolar concentrations in rat brain tissue [21]. Many research groups have not identified the masses measured during tissue imaging experiments, but merely profiled them or compared peak lists generated by MALDI-MSI and LC-MALDI experiments. To demonstrate our ability to truly detect endogenous proteins from tissue, we used MS/MS directly on the tissue sections and identified for example peptide VVSTHEQVLR from human Keratin, type I cytoskeletal 14 (Fig. 5).

We used this systematic approach to optimize our experimental workflow, by evaluating different methods of reagent deposition, and also imaging our samples on a different mass spectrometer (Bruker ultrafleXtreme™) (Supporting Information Fig. S1].

Although we were so far unsuccessful at significantly improving the workflow, we believe that such systematic approach can improve all aspects of the experiment, to achieve the improvement in protein detection required for clinical biomarker discovery.

The estimated sensitivity of MALDI-MSI provides an important baseline for further studies. Many proteins that are currently used as therapeutic or imaging targets are not usually present in high enough concentrations (micro-millimolar) to be visualized by MALDI-MSI. As mentioned

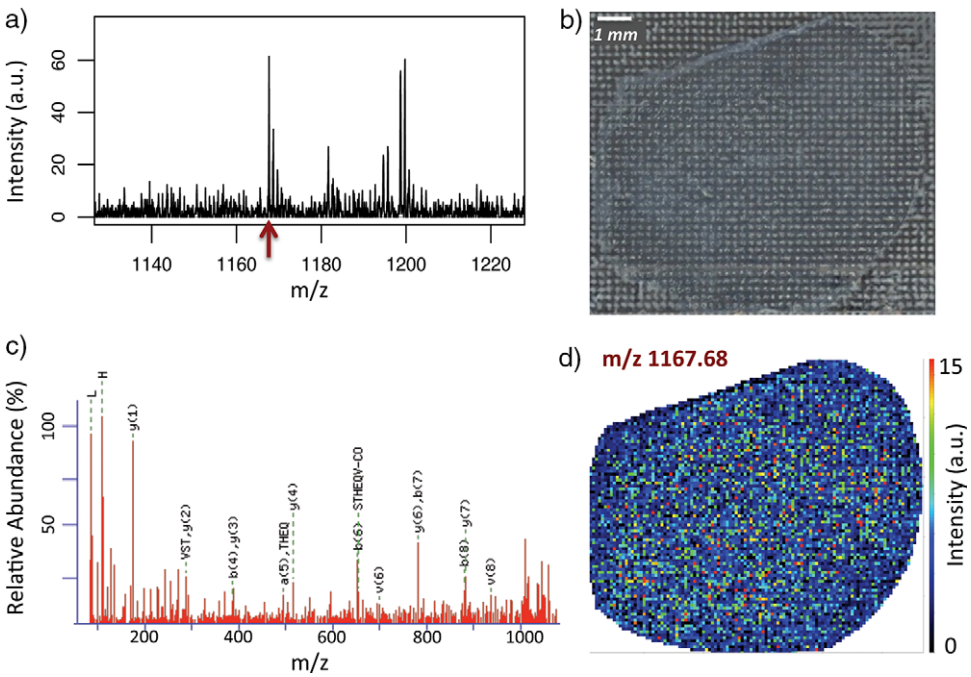

Figure 5. Endogenous protein identification. MALDI-MSI was performed directly on A431 tissue sections after in situ tryptic digestion and matrix deposition. MS peaks of *m/z* 1167.68 were detected on tissue (a); a digital scan shows the tissue section after reagent deposition (b); MS/MS fragmentation of *m/z* 1167.68 on tissue confirmed the identity of endogenous human Keratin, type I cytoskeletal 14 peptide VVSTHEQVLR by Mascot search (c); MALDI ion extraction image exported from CARDINAL software shows the spatial distribution of m/z 1167.68 in the A431 tissue section (d).

Table 3. Overview of MALDI-MS tissue imaging performance evaluation

Criteria	Findings
Limit of detection	μM–mM
Variation	5–30%
Spatial resolution	200–360 μm
Protein identification	Top 10% abundant proteins

before, EGFR expression is 2.8 million per cell in a highly expressing epidermoid carcinoma (A431) cell line, but this is not sufficient to be detectable, unless > 1,700 cells would be present in one spot, which is physically impossible. Other cell lines have lower EGFR expression, i.e. 1.7 million receptors per cell in glioblastoma cells (U87-MGSH mutant EGFRvIII transfected) and 0.17 million in cervical adenocarcinoma (Hela) cells [28]. In a clinical set of 18 breast tumors, HER2 levels in number of receptors per cell were found to range from 11,500 to 584,000; EGFR levels ranged from 220 to 35,500 [31]. Considering these numbers, the sensitivity of MALDI-MSI needs to be improved significantly to allow for the detection of these proteins of interest in tissue.

Sensitivity of MALDI-MSI could be improved by factors as modified tissue preparation [32], alteration of the matrix, advances in mass spectrometers, improved computational processing methods [33], and other targeted imaging approaches using specific antibodies [34, 35], or MRM [21].

In conclusion, the limited sensitivity is currently a major barrier in the discovery of new candidate protein biomarkers from tissue using MALDI-MSI. Using the benchmarking strategy presented above, it may be possible to readily compare approaches and thereby significantly improve current workflows.

We thank Dr. R.H. Kimura for providing the A431 mouse xenograft tissues. This work was supported in part by the NSF CAREER award DBI-1054826 to O.V., the Early Detection Research Network (EDRN) of the National Cancer Institute (NCI) grant U01CA152737, and the Canary Foundation.

The authors have declared no conflicts of interest.

5 References

[1] Cazares, L. H., Troyer, D. A., Wang, B., Drake, R. R., Semmes, O. J., MALDI tissue imaging: from biomarker discovery to clinical applications. *Anal. Bioanal. Chem.* 2011, *401*, 17–27.

[2] McDonnell, L. A., Corthals, G. L., Willems, S. M., van Remoortere, A. et al., Peptide and protein imaging mass spectrometry in cancer research. *J. Proteomics* 2010, *73*, 1921–1944.

[3] Schwamborn, K., Caprioli, R. M., MALDI imaging mass spectrometry–painting molecular pictures. *Mol. Oncol.* 2010, *4*, 529–538.

[4] Eberlin, L. S., Ferreira, C. R., Dill, A. L., Ifa, D. R., Cooks, R. G., Desorption electrospray ionization mass spectrometry for lipid characterization and biological tissue imaging. *Biochim. Biophys. Acta* 2011, *1811*, 946–960.

[5] Kraft, M. L., Klitzing, H. A., Imaging lipids with secondary ion mass spectrometry. *Biochim. Biophys. Acta* 2014, *1841*, 1108–1119.

[6] Schwamborn, K., Krieg, R. C., Reska, M., Jakse, G. et al., Identifying prostate carcinoma by MALDI-Imaging. *Int. J.Mol. Med.* 2007, *20*, 155–159.

[7] Meding, S., Nitsche, U., Balluff, B., Elsner, M. et al., Tumor classification of six common cancer types based on proteomic profiling by MALDI imaging. *J. Proteome Res.* 2012, *11*, 1996–2003.

[8] Gustafsson, J. O., Eddes, J. S., Meding, S., Koudelka, T. et al., Internal calibrants allow high accuracy peptide matching between MALDI imaging MS and LC-MS/MS. *J. Proteomics* 2012, *75*, 5093–5105.

[9] Maier, S. K., Hahne, H., Gholami, A. M., Balluff, B. et al., Comprehensive identification of proteins from MALDI imaging. *Mol. Cell. Proteomics* 2013, *12*, 2901–2910.

[10] Jones, E. E., Powers, T. W., Neely, B. A., Cazares, L. H. et al., MALDI imaging mass spectrometry profiling of proteins and lipids in clear cell renal cell carcinoma. *Proteomics* 2014, *14*, 924–935.

[11] Seeley, E. H., Washington, M. K., Caprioli, R. M., M'Koma, A. E., Proteomic patterns of colonic mucosal tissues delineate Crohn's colitis and ulcerative colitis. *Proteomics Clin. Appl.* 2013, *7*, 541–549.

[12] Lazova, R., Seeley, E. H., Keenan, M., Gueorguieva, R., Caprioli, R. M., Imaging mass spectrometry–a new and promising method to differentiate Spitz nevi from Spitzoid malignant melanomas. *Am. J. Dermatopathol.* 2012, *34*, 82–90.

[13] Hardesty, W. M., Kelley, M. C., Mi, D., Low, R. L., Caprioli, R. M., Protein signatures for survival and recurrence in metastatic melanoma. *J. Proteomics* 2011, *74*, 1002–1014.

[14] Casadonte, R., Kriegsmann, M., Zweynert, F., Friedrich, K. et al., Imaging mass spectrometry to discriminate breast from pancreatic cancer metastasis in formalin-fixed paraffin-embedded tissues. *Proteomics* 2014, *14*, 956–964.

[15] Marquardt, C., Tolstik, T., Bielecki, C., Kaufmann, R. et al., MALDI imaging-based classification of hepatocellular carcinoma and non-malignant lesions in fibrotic liver tissue. *Z. Gastroenterol.* 2015, *53*, 33–39.

[16] Cillero-Pastor, B., Eijkel, G. B., Blanco, F. J., Heeren, R. M., Protein classification and distribution in osteoarthritic human synovial tissue by matrix-assisted laser desorption ionization mass spectrometry imaging. *Anal. Bioanal. Chem.* 2015, *407*, 2213–2222.

[17] Groseclose, M. R., Castellino, S., A mimetic tissue model for the quantification of drug distributions by MALDI imaging mass spectrometry. *Anal. Chem.* 2013, *85*, 10099–10106.

[18] Hamm, G., Bonnel, D., Legouffe, R., Pamelard, F. et al., Quantitative mass spectrometry imaging of propranolol and olanzapine using tissue extinction calculation as normalization factor. *J. Proteomics* 2012, *75*, 4952–4961.

[19] Koeniger, S. L., Talaty, N., Luo, Y., Ready, D. et al., A quantitation method for mass spectrometry imaging. *Rapid Commun. Mass Spectrom.* 2011, *25*, 503–510.

[20] Pirman, D. A., Reich, R. F., Kiss, A., Heeren, R. M., Yost, R. A., Quantitative MALDI tandem mass spectrometric imaging of cocaine from brain tissue with a deuterated internal standard. *Anal. Chem.* 2013, *85*, 1081–1089.

[21] Clemis, E. J., Smith, D. S., Camenzind, A. G., Danell, R. M. et al., Quantitation of spatially-localized proteins in tissue samples using MALDI-MRM imaging. *Anal. Chem.* 2012, *84*, 3514–3522.

[22] Kimura, R. H., Teed, R., Hackel, B. J., Pysz, M. A. et al., Pharmacokinetically stabilized cystine knot peptides that bind alpha-v-beta-6 integrin with single-digit nanomolar affinities for detection of pancreatic cancer. *Clin. Cancer Res.* 2012, *18*, 839–849.

[23] Seeley, E. H., Oppenheimer, S. R., Mi, D., Chaurand, P., Caprioli, R. M., Enhancement of protein sensitivity for MALDI imaging mass spectrometry after chemical treatment of tissue sections. *J. Am. Soc. Mass Spectrom.* 2008, *19*, 1069–1077.

[24] Aerni, H. R., Cornett, D. S., Caprioli, R. M., Automated acoustic matrix deposition for MALDI sample preparation. *Anal. Chem.* 2006, *78*, 827–834.

[25] Casadonte, R., Caprioli, R. M., Proteomic analysis of formalin-fixed paraffin-embedded tissue by MALDI imaging mass spectrometry. *Nat. Protoc.* 2011, *6*, 1695–1709.

[26] Bemis, K., Harry, A., Eberlin, L. S., Ferreira, C et al., Cardinal: an R package for statistical analysis of mass spectrometry-based imaging experiments. *Bioinformatics* 2015, *31*, 2418–2420.

[27] Roskams, J., Rodgers, L., *Lab Ref: A Handbook of Recipes, Reagents, and Other Reference Tools for Use at the Bench*, Cold Spring Harbor Laboratory Press, New York 2002.

[28] Spangler, J. B., Neil, J. R., Abramovitch, S., Yarden, Y. et al., Combination antibody treatment down-regulates epidermal growth factor receptor by inhibiting endosomal recycling. *Proc. Natl. Acad. Sci. U. S. A.* 2010, *107*, 13252–13257.

[29] Cole, L. M., Djidja, M. C., Bluff, J., Claude, E. et al., Investigation of protein induction in tumour vascular targeted strategies by MALDI MSI. *Methods* 2011, *54*, 442–453.

[30] Min, K. W., Bang, J. Y., Kim, K. P., Kim, W. S. et al., Imaging mass spectrometry in papillary thyroid carcinoma for the identification and validation of biomarker proteins. *J. Korean Med. Sci.* 2014, *29*, 934–940.

[31] Ho-Pun-Cheung, A., Bazin, H., Gaborit, N., Larbouret, C. et al., Quantification of HER expression and dimerization in patients' tumor samples using time-resolved Forster resonance energy transfer. *PloS One* 2012, *7*, e37065.

[32] Grey, A. C., Chaurand, P., Caprioli, R. M., Schey, K. L., MALDI imaging mass spectrometry of integral membrane proteins from ocular lens and retinal tissue. *J. Proteome Res.* 2009, *8*, 3278–3283.

[33] Schwartz, M., Meyer, B., Wirnitzer, B., Hopf, C., Standardized processing of MALDI imaging raw data for enhancement of weak analyte signals in mouse models of gastric cancer and Alzheimer's disease. *Anal. Bioanal. Chem.* 2015, *407*, 2255–2264.

[34] Anderson, N. L., Anderson, N. G., Haines, L. R., Hardie, D. B. et al., Mass spectrometric quantitation of peptides and proteins using Stable Isotope Standards and Capture by Anti-Peptide Antibodies (SISCAPA). *J. Proteome Res.* 2004, *3*, 235–244.

[35] Wang, H., DeGnore, J. P., Kelly, B. D., True, J. et al., A technique for relative quantitation of cancer biomarkers in formalin-fixed, paraffin-embedded (FFPE) tissue using stable-isotope-label based mass spectrometry imaging (SILMSI). *J. Mass Spectrom.* 2015, *50*, 1088–1095.

